

#### §4. Improvement of the Design of a Vacuum Pumping System for the Closed Helical Divertor in LHD

Shoji, M.

Two test modules for the closed helical divertor (CHD) have been installed in the inboard side of the torus from the 14th experimental campaign. Compression of neutral particle pressure by more than one-order of magnitude was successfully achieved in the closed divertor region (behind a dome structure) compared to that in the open divertor region for a typical magnetic configuration ( $R_{ax}=3.60m$ ). In the next experimental campaign, a vacuum pumping system for the CHD will be installed behind the dome for the one-helical pitch angle ( $0^\circ < \phi < 36^\circ$ ) along the space between two helical coils for effective particle pumping in the plasma periphery.

For the one of the candidates for the design of the pumping system, a cryogenic adsorption panel cooled by gas helium was proposed. The panel is protected by liquid nitrogen ( $LN_2$ ) cooled chevrons which is covered with water cooled (WC) blinds for protecting the components of the pumping system from the heat load from divertor plates. There are two physical mechanisms of heat transfer from the divertor plates to the adsorption panel. Heat load calculations using a finite element method based software for multi-physics analysis (ANSYS) indicated that the total head load by radiation onto the adsorption panel is  $\sim 30W$  for the full torus geometry. Heat loads on the components of the pumping system by thermal conduction due to neutral particles released from the divertor plates were calculated using a neutral particle transport simulation code (EIRENE) It showed that installation of buffer plates (made of carbon), on which many grooves are scratched on the surface of the

$LN_2$  cooled chevrons, and the WC blinds and the inner vacuum vessel, is effective to reduce the heat load by thermal conduction without serious degradation of the pumping efficiency.

For further improvement of the design of the pumping system, the effect of modification of the configuration of the WC components and the shape of the dome structure is investigated using the neutral transport simulation code. Figure 1 shows four candidates of the modified configuration of the pumping system. Type I is the original one proposed in the last year. Type II is a configuration with an enlarged inlet of the WC blinds with a small dome structure for efficiently taking in neutral particles at the front of the divertor plates. Type III is a configuration in which a slit is opened at the bottom plate of the structure for the WC blinds. In the all three configurations, a 50% transparent mesh is mounted inside the WC blinds for protecting the adsorption panel from the micro-wave heating by ECRH, etc.

The calculated heat load by thermal conduction on the WC blinds ( $Q_{WC}$ ), the  $LN_2$  cooled chevrons ( $Q_{LN_2}$ ) and the He cooled adsorption panel ( $Q_{He}$ ) in the Type I, II and III is indicated in Figure 2. The current of neutral particles absorbed on the He cooled panel (pumping efficiency) ( $I_{He}$ ) is also plotted in the figure. In the calculations, the current of neutral particles released from the divertor plates ( $I_{Div}$ ) is set to 1A. The pumping efficiency is enhanced by a factor of about 2 in the Type III configuration compared to that in the Type I. The heat load on the  $LN_2$  cooled chevrons in the Type-III is about ten times larger than that in the Type-I. The heat load on the WC blinds and the He cooled panel is not affected by the change of the configuration. The most right side plots in the figure show the heat loads and the pumping efficiency in the Type-III with buffer plate installed on the surface of the vacuum vessel in the inboard side of the torus. It shows that the buffer plate is very effective to reduce the heat load on the  $LN_2$  cooled chevrons. It is expected that co-deposition layers formed on the surface of the inner vacuum vessel by carbon sputtering on the divertor plate work as the buffer plate.

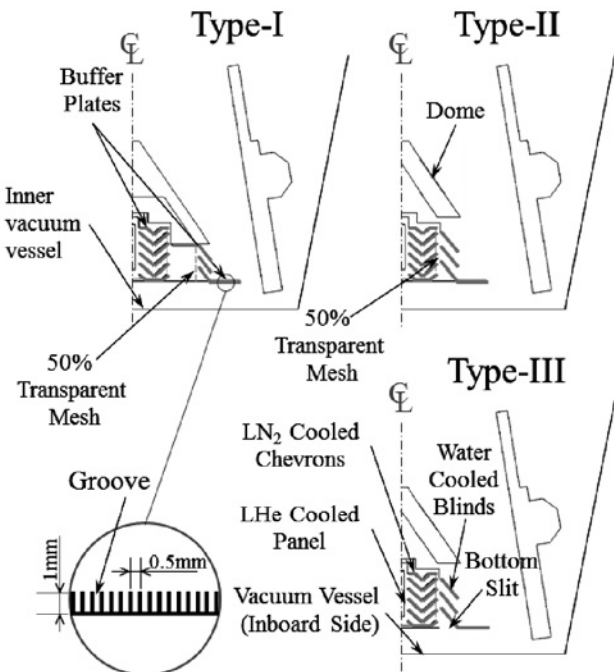


Fig. 1 Cross sections of the three candidates of the configuration of the pumping system for the CHD.

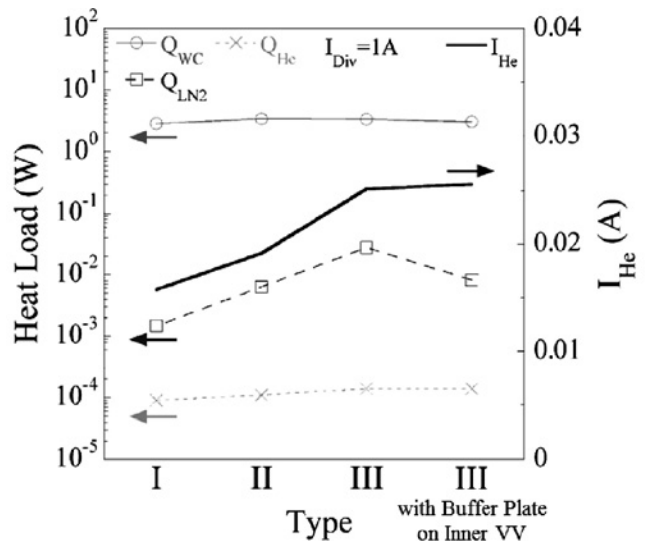


Fig. 2 Calculated heat loads and pumping efficiency in the Type I, II and III configurations.